ELSEVIER

Journal of Crystal Growth 209 (2000) 970–982

JOURNAL OF CRYSTAL GROWTH

www.elsevier.nl/locate/jcrysgro

The influence of convection on the duration of the initial solute transient in alloy crystal growth

J.P. Garandet[a,*], S. Corre[a,1], S. Kaddeche[a,b], T. Alboussière[a,c]

[a]*Commissariat à l'Energie Atomique, DTA/CEREM/DEM/SPCM/LSP, Centre d'Etudes Nucleaires Grenoble, 17 rue des Martyrs, 38054 Grenoble Cedex 9, France*

[b]*INSAT, BP 676, 1080 Tunis Cedex, Tunisia*

[c]*Engineering Department, Cambridge University, Trumpington St., Cambridge CB2 1PZ, England, UK*

Received 2 August 1999; accepted 23 October 1999
Communicated by D.T.J. Hurle

Abstract

Our purpose in this work is to analyse in some detail the influence of convection on the formation and the build-up of the solutal boundary layer during the initial composition transient. Our main assumption is that the alloy is sufficiently dilute for the variation of the interface temperature to be neglected, in other words that the solidification interval is small enough. In order to thoroughly characterise the problem, we use a coupled theoretical (analytical and scaling analysis) and numerical approach. Comparison with existing experimental data is also provided. The effect of convection is seen to be adequately accounted for owing to the convecto-diffusive parameter Δ. The overall agreement observed allows us to propose a simple rule of thumb expression for the extent of the initial composition transient.

Keywords: Solutal transport; Convection; Diffusion; Microgravity; Mephisto program

1. Introduction

In many experimental configurations, an initial transient period is necessary before a solidification steady state can be reached. Such a period was shown for instance to be important in the study of pattern formation [1,2] or to control the morphological stability of the growth front [3]. Regarding solute segregation in alloy crystals, the problem had received a lot of attention in the 1950s, where various analytical solutions were proposed by Tiller et al. [4], Pohl [5] as well as Smith et al. [6] and Memelink [7]. The main assumptions in these studies was that solute transport proceeded only by diffusion and that the interface velocity reached instantaneously its prescribed value. In recent days, the models were refined under the same basic assumptions to account for kinetic undercooling at the growth front [8] and solidification from an initially heterogeneous melt [9]. From a mathematical standpoint, it should also be noted that a rigorous new derivation of the results of Smith et al. was proposed by Nastac [10].

* Corresponding author. Tel.: + 33-476-883663; fax: + 33-476-885117.

E-mail address: garandet@chartreuse.cea.fr (J.P. Garandet)

[1] Present address: Creusot-Loire Industrie, BP 56, 71 202 Le Creusot Cedex, France

0022-0248/00/$ - see front matter
PII: S0022-0248(99)00630-2

Nomenclature

A	aspect ratio of fluid cavity for numerical simulations
C	solute composition field (mass fraction)
C_0	nominal solute composition (mass fraction)
C_S	solid state interface composition in 1-D analytical approach (mass fraction)
$C_{S,Av}$	average solid state interface composition in numerical simulations (mass fraction)
C_{SS}	steady state solid state interface composition (mass fraction)
D	solute diffusion coefficient ($m^2\ s^{-1}$)
e	rejected solute loss to bulk fluid (mass fraction)
Gl	liquid phase temperature gradient ($K\ m^{-1}$)
g	gravity ($m\ s^{-2}$)
H	typical dimension of the fluid cavity (m)
k	equilibrium partition coefficient
k_{eff}	effective partition coefficient
t_T	initial transient duration (s)
V	fluid velocity ($m\ s^{-1}$)
V_{eff}	effective solute transport velocity ($m\ s^{-1}$)
V_I	interface velocity ($m\ s^{-1}$)
Z_T	initial transient length (m)
z	nondimensional coordinate along crystal axis ($z = ZV_I/D$)

Greek

β_T	thermal expansion coefficient (K^{-1})
δ	solutal boundary layer thickness (m)
Δ	convecto-diffusive parameter ($\Delta = \delta V_I/D$)
Δc	normalised radial segregation ($\Delta c = \Delta C/C_{S,Av}$)
v	kinematic viscosity ($m^2\ s^{-1}$)

Nondimensional numbers

Gr	Grashof number ($Gr = \beta GlgH^4/v^2$)
Pe	Peclet number ($Pe = HV_I/D$)
Sc	Schmidt number ($Sc = v/D$)

Warren and Langer [11], as well as Caroli et al. [12], addressed the problem of interface recoil, in other words the fact that the front temperature changes during the initial transient, due to local composition variations. Indeed, considering the relatively low velocities used in conventional solidification, a quasi-equilibrium can be assumed at the solid–liquid interface, meaning that there will be a direct correlation between temperature and concentration changes. Such an effect is expected to be important at high values of $\Delta T_0/G$, where ΔT_0 represents the solidification interval at a given alloy composition C_0 and G the thermal gradient, as checked by Huang et al. [13]. An assumption common to all these models is that the thermal transient necessary for the heat transfer within the furnace is very short [12], but we shall see in the experimental section that this hypothesis may be questionable.

Comparatively, little attention has been paid to the role of fluid flow in the formation of the solute boundary layer ahead of the growth front, even though most solidification processes take place in the presence of convection. Using the stagnant film model initially proposed by Burton et al. [14], Huang et al. obtained a numerical solution for the composition variations in a sample of finite length. Such an approach had been used earlier by Favier [15], who obtained a solution in the form of an asymptotic series. However, the lack of physical basis of the stagnant film representation has been criticised in standard literature works [16–18]; it thus seemed interesting to see whether the solute boundary layer model, initially proposed by Wagner [19] and later revived by Wilson [20], could account for the effect of convection on the duration of the initial transient.

Our focus in the present work will be to examine in some detail the role of convection in the phases of formation and build-up of the solute boundary layer from an initially homogeneous melt. We shall not consider the interface recoil, and assume that

the interface velocity jumps instantaneously to its prescribed value. Our purpose will be to provide exact (Section 2) and approximate (Section 3) analytical solutions for the composition variations in the initial transient, expected to be physically relevant for experimental conditions such that the ratio $\Delta T_0/G$ is low and the thermal transients are short. The validity of these solutions will be checked by means of numerical simulations (Section 4) and by comparison with existing experimental data (Section 5). These results will allow one to propose a rule of thumb expression for the duration of the solute boundary layer build-up, that can be easily used in practice.

2. Analytical solution

Our starting point will be the classical convecto-diffusive equation governing solute conservation in a binary alloy, written in a frame moving at the interface velocity V_I. The rationale behind this choice of reference frame is that it allows a steady state to be reached, after an initial transient that we plan to derive. If we let C, D and $\boldsymbol{V}$ stand, respectively, for the alloy composition, solute diffusion coefficient and convection velocity, the equation can be written as

$$\partial C/\partial t + (\boldsymbol{V}\cdot\nabla)C = D\nabla^2 C + (\boldsymbol{V}_I\cdot\nabla)C. \tag{1}$$

In the frame of the boundary layer model, assuming that the relevant composition variations take place in the Z-direction, the above equation becomes [18,21]

$$\partial C/\partial t = D\partial^2 C/\partial Z^2 + V_{\mathrm{eff}}\partial C/\partial Z, \tag{2}$$

where the constant effective velocity V_{eff} is defined as D/δ, δ being the steady-state solute boundary layer thickness. This effective velocity accounts for the combination of both diffusive and convective mass transport [21]. The validity of the formulation has been successfully tested in a variety of situations [18,22]. An implicit assumption in Eq. (2) is that the boundary layer thickness has reached its steady-state extent δ in a time that is short compared to the total duration of the initial transient. In other words, we suppose that the filling-up of the boundary layer is the limiting kinetic process, but we shall check the validity of this assumption in the scaling analyses carried out in Section 3.

To fully specify the mass transport problem, we need initial and boundary conditions. We shall assume that at $t = 0$, the melt is at uniform composition

$$C = C_0 \quad \text{at } t = 0. \tag{3}$$

In a dilute alloy with a constant partition coefficient k, solute conservation at the interface takes the form

$$-D(\partial C/\partial Z)_I = V_I(1-k)C_I. \tag{4}$$

As for the far field condition, we shall assume that the composition remains equal to its initial value

$$C \to C_0 \quad \text{when } Z \to \infty. \tag{5}$$

We are thus left with a linear equation with constant coefficients, that can be solved using a Laplace transform technique, initially proposed in Refs. [6,7]. The interested reader is referred to the Appendix for the details of the derivation. The composition profile can be expressed as a function of the nondimensional parameter $\Delta = \delta V_I/D$ that measures the relative importance of diffusive and convective mass transport. This parameter Δ ranges from values close to zero in the case of strong fluid flows to unity for purely diffusive mass transport. In the following, we shall refer to Δ as the convecto-diffusive parameter [18]. Equivalently, composition profiles can be characterised by the effective partition coefficient k_{eff}, defined as C_{SS}/C_0, C_{SS} being the steady-state composition in the solid. The effective partition coefficient k_{eff} will range between k (total mixing in the melt) and unity (purely diffusive mass transport). More specifically, the relation between the effective partition coefficient and the convecto-diffusive parameter can be written as [18]

$$k_{\mathrm{eff}} = k/[1-(1-k)\Delta]. \tag{6}$$

Setting $q = (1-k)$ and defining the nondimensional distance z as $z = ZV_I/D$, the solid state

composition profile can be expressed as

$$C_S(z) = \frac{1}{2}k_{eff}C_0\left\{1 + \mathrm{erf}\left[\frac{\sqrt{z}}{2\Delta}\right] + (1 - 2q\Delta)e^{-(1-q\Delta)qz/\Delta} \times \mathrm{erfc}\left[\frac{(2(1-q\Delta)-1)\sqrt{z}}{2\Delta}\right]\right\}. \quad (7)$$

The effect of convection is thus taken into account through the convecto-diffusive parameter Δ. Our final closed form result appears relatively simple compared to Huang's numerical formulation [13] or to Favier's series expansion [15]. However, we shall now see that it can be further amended owing to the scaling analyses of next section.

3. Scaling analysis arguments

The developments of this section will be based on the physical assumption that the initial transient consists of two stages: in the "formation" stage, the extent of the established liquid-phase composition gradient will rise from zero (homogeneous fluid) to δ, the thickness of the steady-state boundary layer. Later, in the "filling-up" stage, the interface composition will increase to reach its final value, C_{SS}/k. Depending on the kinetics of both processes, different assumptions will be made. We shall first consider the case where the initial transient duration is governed by the filling up of the solute boundary layer.

3.1. "*Filling-up*" *limited kinetics*

The boundary layer having reached its steady-state extent, it is reasonable to assume that the rate of solute loss through the boundary layer towards the bulk fluid is proportional to $C_S/k - C_0$, in other words to the instantaneous composition difference between the interface and infinity. We shall see that such a hypothesis is essentially equivalent to that made by Tiller et al. [4] in the case of diffusion-controlled solute transport. Denoting e as the amount of solute that escapes per unit of length solidified, we can write

$$e = \gamma(C_S - kC_0), \quad (8)$$

where the proportionality constant γ can be derived using the fact that at steady state, i.e. when $C_S = C_{SS}$, e is equal to $C_0 - C_{SS}$. Indeed, at steady state, a solid of composition C_{SS} forms from a liquid of composition C_0. As both the spatial extent and the amplitude of the composition variations of the boundary layer are fixed, the solute rejected by the advancing interface has to "escape" in the bulk fluid. We thus get

$$\gamma = (C_0 - C_{SS})/(C_{SS} - kC_0). \quad (9)$$

We can now write that when the interface is at the abscissa Z, the amount of solute inside the boundary layer Q is equal to the total amount rejected since the beginning of solidification ($Z = 0$) minus the amount that has been lost to the bulk fluid

$$Q = \int_0^Z (C_0 - C_S)\,\mathrm{d}u - \int_0^Z e\,\mathrm{d}u. \quad (10)$$

The amount Q can be estimated by stating that the solute composition in the fluid decreases exponentially from C_S/k at the interface to C_0 in the bulk fluid over a length scale δ

$$Q = \left(\frac{C_S}{k} - C_0\right)\delta. \quad (11)$$

Differentiating Eq. (10) with respect to Z using the expression of Q given by Eq. (11), we obtain a first-order linear differential equation with constant coefficients in terms of C_S

$$\lambda_1\,\mathrm{d}C_S/\mathrm{d}Z + \lambda_2 C_S = \lambda_3 \quad (12)$$

the constants λ_1, λ_2 and λ_3 being given as

$$\lambda_1 = \delta/k, \quad \lambda_2 = C_0(1-k)/(C_{SS} - kC_0),$$
$$\lambda_3 = C_{SS}C_0(1-k)/(C_{SS} - kC_0). \quad (13)$$

Without a priori prescribing the rate of approach towards steady-state conditions, as assumed by Tiller et al. [4] for diffusion-controlled solute transport, we thus find that the kinetics of the initial transient are exponential. The characteristic length

scale for the filling-up of the solutal boundary layer, and thus of the initial transient, can be defined as $Z_T = \lambda_1/\lambda_2$ from the structure of Eq. (12). Plugging in $C_{SS} = k_{eff} C_0$, with k_{eff} given by Eq. (6), we get

$$Z_T = \delta\Delta/[1-(1-k)\Delta]$$
$$= (D/V_I)\Delta^2/[1-(1-k)\Delta]. \quad (14)$$

More precisely, the solution to Eq. (12) yields the composition profile in the solid

$$C_S(Z) = C_{SS}[1-(1-k)\Delta \exp(-Z/Z_T)]. \quad (15)$$

It is interesting to note that, in the limiting cases of diffusion-controlled and highly convective solute transport, Eq. (14) reduces to

$$Z_T = \frac{D}{kV_I} \quad (\Delta = 1), \quad (16)$$

$$Z_T = \frac{D}{V_I}\Delta^2 \quad (\Delta \to 0). \quad (17)$$

Eq. (14) thus accounts for the effect of convection on the duration of the initial transient. However, we now have to check the validity of the "filling-up" limited kinetics assumption: to do so, the time necessary to establish by diffusion a composition gradient over a length scale δ, in other words the "formation time", will be estimated as δ^2/D

$$t_{formation} = \frac{\delta^2}{D} = \frac{D}{V_I^2}\Delta^2.$$

This is to be compared with the "filing-up" time, derived from Eq. (14)

$$t_{filling\text{-}up} = \frac{Z_T}{V_I} = \frac{D}{V_I^2}\frac{\Delta^2}{1-(1-k)\Delta}.$$

The ratio between the "formation" and "filling-up" times is thus given as

$$t_{formation}/t_{filling\text{-}up} = 1-(1-k)\Delta. \quad (18)$$

Such a ratio varies from k for the diffusive transport regime to unity for convective conditions. When $\Delta \to 0$, we shall now see that other solute conservation arguments can be invoked to estimate the duration of the initial transient.

3.2. Simultaneous "formation" and "filling-up"

We shall here assume that, as long as the solutal boundary layer has not reached its final extent δ, all the solute rejected by the advancing interface remains in the vicinity of the growth front. Such an assumption is reasonable, since convection is not efficient in removing the solute at a scale smaller than δ, as shown in Ref. [18]. It is however somewhat drastic, since it amounts to stating that, after the "formation" stage, all the solute escapes to the bulk fluid, whereas it remained in the vicinity of the growth front in the "formation" stage. At the location Z_T of that transition, we can write that enough solute has been rejected to build the steady state boundary layer

$$Q = \int_0^{Z_T} (C_0 - C_S)\,du. \quad (19)$$

The amount Q being again given by Eq. (11) with $C_S = C_{SS}$. In the limit of highly convective solute transport ($\Delta \to 0$), it is licit to assume that during the initial transient, as well as in the steady state, C_S remains close to kC_0. Eq. (19) thus becomes

$$(C_{SS}/k - C_0)\delta = Z_T(1-k)C_0.$$

Or, after simple algebra, plugging in again $C_{SS} = k_{eff} C_0$, with k_{eff} given by Eq. (6)

$$Z_T = \delta\Delta = (D/V_I)\Delta^2. \quad (20)$$

For the sake of consistency, we wrote Eq. (20) in the limit $\Delta \to 0$. To conclude, we find that the prediction of Eqs. (14) and (20) are equivalent in the convective solute transport regime limit. As the underlying physical assumptions are totally different in the two cases, such a result could not have been a priori expected. Even though the convergence of two approximate solutions cannot be taken as a proof of their validity, we shall consider that Eq. (14) can be used whatever the convecto-diffusive state of the melt.

3.3. Validation of the approximate solution

The simple exponential behaviour of Eq. (15) cannot obviously account for the more complex

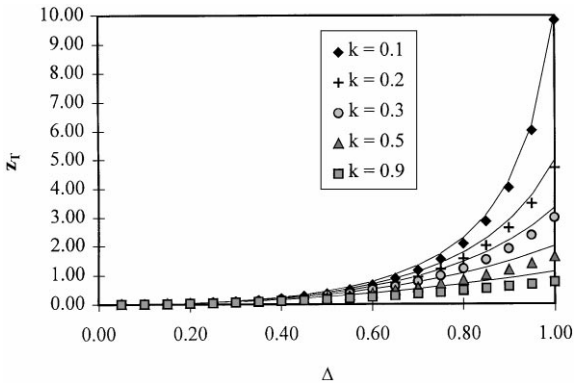

Fig. 1. Variation of the nondimensional initial transient length $z_T = Z_T V_1/D$ with the convecto-diffusive parameter Δ. Comparison of the predictions of the analytical (Eq. (7), symbols) and order of magnitude (Eq. (14), full line) theoretical approaches.

form predicted by Eq. (7). Nevertheless, both composition profiles have the same starting (kC_0) and end (C_{SS}) points. The remaining question is whether the variation predicted by Eq. (7) takes place over a length scale of the order of Z_T. To assess quantitatively the possible discrepancies for a variety of k and Δ values, we computed for both composition profiles the distance where the concentration level reaches $kC_0 + (1 - e^{-1})(C_{SS} - kC_0)$. For the exponential behaviour of Eq. (15), this distance is simply Z_T. The comparison presented in terms of nondimensional values in Fig. 1 shows that the agreement between the two analytical approaches is very good, the maximum discrepancy being of the order of 30%. More precisely, in the convective regime, the characteristic length Z_T of the initial transient computed from Eq. (7) is given by

$$Z'_T = 0.7(D/V_1)\Delta^2. \quad (21)$$

It is interesting to note that in this convective regime, Z'_T is independent of the partition coefficient k, in agreement with the predictions of the scaling analysis, as given by Eq. (17). The most striking result of the analytical approaches is that the initial transient is very short, since in many actual growth experiments the convecto-diffusive is fairly small, say $\Delta < 0.3$. We shall now confirm the validity of the analytical approaches with the help of numerical simulations, presented in the next section.

4. Numerical simulations

We first relied on the simulations carried out in Ref. [23], where an idealised Czochralski configuration was numerically modelled. In order to account for the effect of convection, the results were presented in terms of an equivalent stagnant film thickness. It was thus possible to derive the convecto-diffusive parameter Δ for purposes of comparison with our model. Fig. 2 shows the numerical composition profiles along with those predicted by Eq. (7). The agreement can be considered very good, the maximum error being of the order of 8%. Nevertheless, due to the relatively low number of cases simulated, no definite conclusion regarding the validity of our analytical approaches could be drawn. That is why we decided to perform dedicated numerical simulations to carry out a parametric study.

To assess the capacity of the convecto-diffusive parameter to account for the effect of convection, both a horizontal and a vertical Bridgman configurations were modelled. The governing equations were solved using an alternating direction implicit (ADI) technique, with a finite-difference method involving forward differences for time derivatives and Hermitian relationships for spatial derivatives, resulting in a truncation error of the second and fourth orders in $O(\Delta t^2, \Delta r^4)$ for time and space steps respectively (see Hirsh [24] and Roux et al. [25]). The mesh used to solve the problem was generated by Thompson technique [26]. The node density is of course larger near the side walls of the

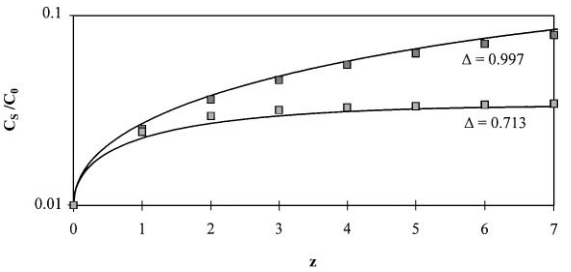

Fig. 2. Axial composition profiles versus nondimensional distance $z = ZV_1/D$, as computed from Eq. (7) (full line) and resulting from the numerical simulations of Favier and Wilson (symbols). The equilibrium partition coefficient k was taken to be equal to 0.01.

cavity, especially in the vicinity of the growth interface. A 25×101 grid was found to guarantee a sufficient accuracy for such studies, as shown in Refs. [27,28] where the details of the numerical procedure are presented.

Regarding physical assumptions, only thermal convection was considered (dilute alloy approximation). In both cases, the numerical approach was two-dimensional, respectively cartesian and axisymmetric for the horizontal and vertical problems. A vorticity–stream function formulation was used for the hydrodynamic field. In addition to the partition coefficient k, the nondimensional parameters of the problem were:

- the Grashof number, $\mathrm{Gr} = \beta_T GlgH^4/v^2$, characterising the convection driving force; its definition features the thermal expansion coefficient β_T, the liquid phase temperature gradient Gl normal to the gravity vector g, a sample macroscopic dimension H and the cinematic viscosity of the fluid v.
- the Schmidt number $\mathrm{Sc} = v/D$, measuring the ratio of the momentum and species diffusivities.
- the Peclet number $\mathrm{Pe} = HV_I/D$, scaling the growth velocity.

Axial and radial solute segregation were, respectively, characterised by the average composition on slices taken normal to the growth direction $C_{S,Av}$ and by the normalised composition difference along the interface Δc, defined as

$$\Delta c = (C_{S,Max} - C_{S,min})/C_{S,Av} \quad (22)$$

the quantities $C_{S,Max}$ and $C_{S,min}$ representing, respectively, the maximum and the minimum of the concentration at a given location of the interface.

A characteristic of all the numerical simulations performed was that the initial elongation ratio was relatively small, $A = 4$. As opposed to the work conditions of Favier and Wilson [23], no true steady-state composition plateau could be reached in our simulations, and we had to design a new strategy to estimate the characteristic length scale of the initial transient. To do so, we took advantage of the structure of the normalised radial segregation profiles: these were found to start from zero (homogeneous melt initial condition), and increase to a maximum value Δc^M lying just above a fairly well-defined plateau value (see Fig. 3).

The location of this maximum Δc^M was shown to correspond to the inflexion point in the axial segregation profiles, and we thus defined the characteristic length scale of the initial transient Z_T as the point where the radial concentration reached the value $(1 - e^{-1})\Delta c^M$. It should be noted that the coincidence between $C_{S,Av}$ and Δc in terms of steady-state attainment rate cannot at this point be explained by simple scaling analysis arguments. It is, nevertheless, an interesting result of the numerical simulations that the initial transient duration is the same for both axial and radial segregations.

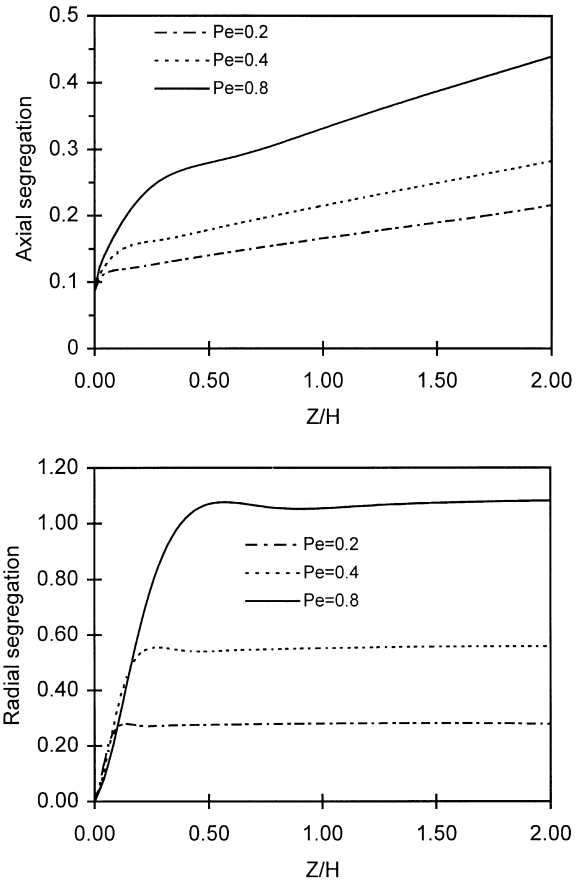

Fig. 3. Typical radial and axial segregation profiles obtained from our numerical simulations, demonstrating the correspondence between the inflexion point of $C_{S,Av}$ and the maximum in Δc. The equilibrium partition coefficient k was taken to be equal to 0.087.

Overall, a very good agreement was observed between the simulation results and the theoretical predictions of Section 3. Special emphasis was laid on the convective solute transport limit, since it is the most important in experimental practice. The analysis of the numerical segregation profiles shows that Z_T/H is independent of the partition coefficient k and varies linearly with the Peclet number in the low Δ range. This can be understood from Eq. (17), that can be rewritten as $Z_T/H = \Delta^2/\mathrm{Pe}$, and from the fact that Δ is proportional to Pe in the convective solute transport limit [18].

The variation of Z_T/H with the Grashof and Schmidt number is more intricate, but the results can be nicely interpreted if the convecto-diffusive parameter Δ is computed for each simulation. Indeed, as can be seen in Fig. 4, the numerical results for both the vertical and the horizontal configurations are found to be smoothly fitted by a parabolic law in accordance with Eq. (17). However, the proportionality constants ξ in the $Z_T/H \sim \xi\Delta^2$ power law are slightly different, namely $\xi = 1.6$ for vertical Bridgman and $\xi = 1.8$ for horizontal Bridgman. This means that the convecto-diffusive parameter Δ cannot by itself account for all the details of transient solute incorporation.

Nevertheless, the fact that the proportionality constants are both close to each other and close to unity supports the validity of the scaling analysis of Section 3. Our numerical results also support the ability of the convecto-diffusive parameter Δ to capture the main physics of the mass transport phenomena in the melt, as already observed in a variety of related problems [21,22]. In any case, an important consequence of the above results is that, for the case usually met in practice where the convecto-diffusive parameter is small, the initial transient related to the solutal boundary layer will be very short. We shall see in the next section that this is indeed the case for most of the available experimental results.

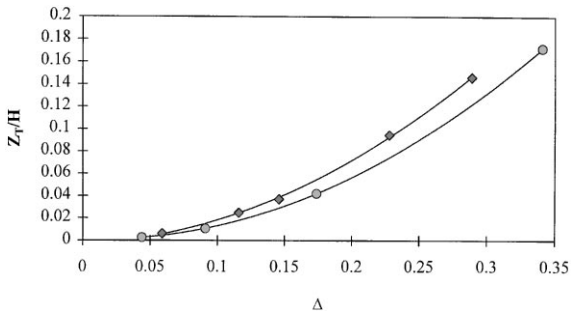

Fig. 4. Summary of numerical results showing the variation of the extent of the initial transient with the convecto-diffusive parameter Δ for both horizontal (squares) and vertical (circles) Bridgman configurations.

5. Comparison with experimental data

In addition to numerical results, we also wanted to check the validity of our scaling analysis results with existing experimental data. However, for the comparison to be meaningful, the growth conditions have to be sufficiently well specified for the derivation of the convecto-diffusive parameter. For instance, we cannot analyse the segregation profiles of Inatomi et al. [29] in our theoretical frame. Besides, due to our starting assumptions, Eq. (14) is only expected to be valid for experimental conditions such that the ratio $\Delta T_0/G$ is low, so that the interface recoil problem can be bypassed. This means that our focus will be on dilute alloys, but our approach is expected to stand in concentrated systems in the case where convective transport keeps the solidification interval ΔT_0 low enough. With all these constraints in mind, we mostly relied on experiments carried out in the Mephisto furnace facility on tin-based alloys, both on the ground and in microgravity [30,31], but we were also able to analyse the works of Helmers et al. [32,33] on GeSi mixed crystals.

5.1. Mephisto results

Mephisto is essentially a sophisticated Bridgman furnace developed in cooperation between the French space (CNES) and nuclear (CEA) national research agencies. It is equipped with a variety of diagnostics, including resistance measurements and Peltier pulsing. Of particular interest for the present work is the possibility to measure the instantaneous composition at the growth interface using the thermoelectric Seebeck signal. Without going

into details (see e.g. Refs. [30,31] for more information on the topic), the system acts as a thermocouple that yields the temperature and, by means of the phase diagram, the concentration at the solidification front. The measurement is both on line and in situ and is thus particularly well suited for the study of segregation phenomena.

A series of experiments was carried out on the ground in a horizontal configuration. Various growth velocities V_I, ranging from 0.3 to 1.1 mm/min, were used, the crucible diameter and the applied thermal gradient being, respectively, fixed at 6 mm and 130 K/cm. The time variation of the Seebeck signals is shown in Fig. 5; as the Seebeck measurement is differential in nature [30], its value at the onset of solidification (here $t = 300$ s) is strictly zero. The signals then increase up to a plateau value V_P, and we shall take for the experimental initial transient duration the time t_T^{exp} where the Seebeck reaches the value $(1 - e^{-1})V_P$. Using Eq. (6), this plateau value V_P can also be used to derive the value of the convecto-diffusive parameter Δ, and thus to estimate analytically the initial transient duration $t_T^{ana} = Z_T/V_I$, Z_T being computed from Eq. (14). As commonly found in horizontal configurations on earth, the convecto-diffusive parameter increases with the pulling velocity, but remains smaller than 0.5 even at the fairly large growth rate of 1.1 mm/min.

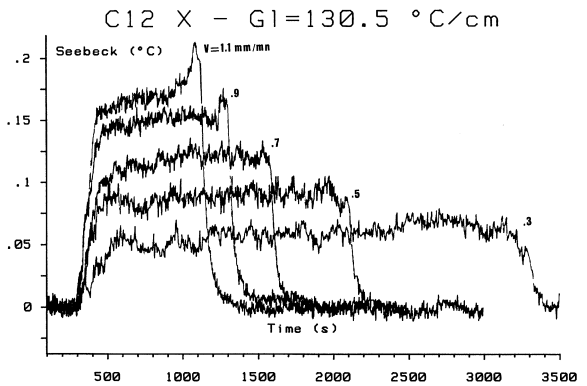

Fig. 5. Time variation of the Seebeck signals at growth velocities ranging from 0.3 mm/min to 1.1 mm/min. In all cases, the onset of solidification is at $t = 300$ s.

The results are summarised in Table 1, where it can be seen that t_T^{exp} is always much higher than t_T^{ana}. Such a finding can be explained by the fact that the thermal lag of the furnace, experimentally found to be in the 100 s range [31], is much higher than the time necessary to form and fill the solutal boundary layer. It should be noted that such a thermal lag is short compared to those of classical furnaces, where values of the order of 1000 s are not uncommon, but the Mephisto facility is equipped with liquid metal rings in the cold zone that ensure an efficient contact with the water-cooled sink. This allows an efficient heat extraction, and thus a short thermal lag time. As the growth velocity only reaches its prescribed values over a thermal lag time scale, the latter controls the kinetics of the initial composition transient. For the sake of completeness, it should be mentioned that repeated solidification cycles in the $V_I = 0.3$ mm/min experiment show that the t_T^{exp} is more likely to be of the order of 120 s (see Fig. 4 of Ref. [30]) The thermal lag time of the furnace is thus found to be roughly independent of the pulling velocity.

In microgravity, the results of the USMP1 flight of the Mephisto facility in 1992 showed that diffusion-controlled solute transport conditions were reached at growth velocities higher than $V_I = 0.12$ mm/min. The fit of the initial composition transient allowed to check the coherence of the parameters data set [31], and especially of the diffusion and partition coefficients of bismuth in tin, estimated at $D = 1.3 \times 10^{-9}$ m^2/s and $k = 0.27$, respectively. Lower growth velocities were used during the USMP3 mission in 1996, and a slight

Table 1
Experimentally determined convecto-diffusive parameter Δ and characteristic duration of initial transient t_T^{exp} in Mephisto ground experiments, along with comparison to predicted values from Eq. (14)

V_I (mm/min)	Δ	t_T^{exp} (s)	Z_T^{ana} (μm)	t_T^{ana} (s)
0.3	0.19	145	11	2.3
0.5	0.31	106	20	2.4
0.7	0.39	117	24	2
0.9	0.46	83	28	1.9
1.1	0.5	83	27	1.5

convective interference was observed at the lowest growth velocity $V_I = 0.03$ mm/mn. Indeed, the concentration plateau was located at 1.3 at%. Bi, for a nominal alloy composition of 1.6 at% Bi, leading to a value of the convecto-diffusive parameter Δ of 0.91.

The distance where the concentration level reached $kC_0 + (1 - e^{-1})(C_{SS} - kC_0)$ was found to be of the order of 5 mm, whereas the value D/kV_I predicted by Tiller et al. [4] for purely diffusive solute transport is about 9.6 mm. Our analytical expression (Eq. (14)) yields a value of $Z_T = 6.4$ mm, and allows to account semi-quantitatively for the shortening of the initial transient. Experimentally, the characteristic duration t_T in that case is of the order of 10 000 s, and is thus much higher than the thermal lag time of the furnace. From a practical point of view, it should be noted that, even for a value of the convecto-diffusive parameter Δ close to unity, residual convection leads to a significant reduction of the initial transient length with respect to the diffusive transport D/kV_I value.

5.2. Helmers et al. results

In their attempts to grow $Ge_{1-x}Si_x$ mixed crystals of various compositions by the vertical Bridgman technique, Helmers et al. [32,33] were led to analyse the observed initial composition transients. Of particular interest for our present work was the fact that the solidification conditions were sufficiently well defined for the derivation of the relevant nondimensional numbers. Due to the large composition variations along the crystals, some thermophysical and growth parameters, such as partition coefficient, thermal gradient, could not be taken as uniform. However, since the observed initial transients are very short, of the order of 15 μm, we can safely consider that only the conditions at the onset of solidification are to be considered.

A questionable claim made by Helmers et al. [32] is that the diffusion boundary layer and the initial transient are necessarily of the same extent. In our notations, this means that Z_T would be equal to δ, but such a statement is clearly in contradiction with our theoretical and numerical results. Besides, if we follow Helmers et al., the boundary layer thickness would be only of circa 15 μm. This is in contradiction with a number of literature results on vertical Bridgman growth (see e.g. [28,34–36]) where δ is seen to be much larger. Our opinion is that the results of Helmers et al. can be explained using Eq. (14) for the initial transient along with the expression proposed in Ref. [28] for the convecto-diffusive parameter in the convective regime limit

$$\Delta = 13.2\ \mathrm{Pe}(\mathrm{Gr}_{\mathrm{eff}}\mathrm{Sc})^{-1/3}, \tag{23}$$

where Gr_{eff} is the effective Grashof number based on the radial temperature gradient, i.e. on the true driving force for convective motion. Taking the sample radius (5.5 mm), the growth velocity (1 mm/h) and the radial temperature gradient (20 K/cm), along with the values of the thermophysical parameters, from the paper of Helmers et al., we get:

$$\mathrm{Pe} = 5.9 \times 10^{-2}, \quad \mathrm{Gr}_{\mathrm{eff}} = 27\,100, \quad \mathrm{Sc} = 10.4.$$

Plugging these values in Eq. (23), we find $\Delta = 1.2 \times 10^{-2}$. Incidentally, at such a low value of the convecto-diffusive parameter, convection is clearly the dominant solute transport mode, justifying the use of Eq. (23). It should also be noted that this value of Δ translates into a dimensional boundary layer thickness $\delta = 1.1$ mm, typical of vertical Bridgman growth. If we now turn to Eq. (14) to estimate the initial transient duration, we get $Z_T = 13$ μm, in unexpectedly good agreement with the experimental result, $Z_T = 15$ μm.

One should keep in mind that we deliberately neglected the solutal stabilisation mechanism. Our opinion is that, due to the limited extent of the solutal boundary layer thickness where the relevant composition gradient exists, the effect should not be very strong. Besides, it should also be noted that the initial transient duration, derived from $Z_T = 15$ μm and $V_I = 1$ mm/h is of the order of 50 s. It may well be that the thermal lag time of the furnace is in that range, but no indication is given in the original paper to draw a definite conclusion. In any case, we strongly believe that $Z_T = 15$ μm should not be taken as the solutal boundary layer thickness, and we think that a coherent picture of the

experimental results emerges from our theoretical approach.

6. Concluding remarks

Our purpose in the present work was to analyse the effect of convection on the formation and the build-up of the solutal boundary layer. To do so, we adapted the analytical solution first derived by Smith et al. [6] and Memelink [7] under the assumption of negligible interface recoil to account for convective transport. We carried out a scaling analysis of the transport problem to obtain a simple closed-form expression for the initial transient duration. The validity of these theoretical approaches was checked by means of numerical simulations modelling both the horizontal and the vertical Bridgman configurations. We also found that existing experimental data could be interpreted in our theoretical frame. The agreement between the analytical, numerical and experimental results apparent in the present work allows one to propose a rule of thumb expression for the duration of the initial composition transient, that can be easily used in practice. Convection is accounted for in Eq. (14) by means of the steady-state convecto-diffusive parameter Δ, that, in addition to past successes [18,21,22], appears to be one of the keys to the modelling of the initial composition transient in crystal growth from the melt.

An important practical consequence for growth experiments is that the solutal boundary layer formation and build-up is generally extremely short when convection dominates mass transport, say for values of the convecto-diffusive parameter Δ smaller than 0.2. This means that the heat transfer phenomena in the growth furnace will often control the kinetics of the initial composition transient, as was indeed observed in our ground-based experiments. On the other hand, in microgravity conditions where diffusion mostly controls solute transport, the solutal boundary layer formation and build-up will often be much higher than the thermal lag time of the furnace. In any case, a slight departure from purely diffusive conditions results in a significant reduction of the initial transient, as predicted theoretically and checked experimentally during the Mephisto USMP3 experiment.

Acknowledgements

It is a pleasure to thank Pr. H. Ben Hadid and Dr. D. Henry for many fruitful discussions in the course of this work. The contribution of S. Corre and J.P. Garandet is part of the GRAMME agreement between the CNES and the CEA. The contribution of the whole Mephisto team, headed by Dr. J.J. Favier, is also gratefully acknowledged.

Appendix A. Derivation of the analytical solution

Our starting point is the one-dimensional mass conservation equation written in the effective velocity formalism; this means that we implicitly suppose the formation phase of the solutal boundary layer to be small compared to the total length of the initial transient:

$$\frac{\partial C}{\partial t} = D\frac{\partial^2 C}{\partial Z^2} + V_{\text{eff}}\frac{\partial C}{\partial Z}.$$

Introducing the Laplace transform

$$\bar{C}(S) = \int_0^\infty C\mathrm{e}^{-St}\,\mathrm{d}t,$$

we get

$$\frac{\mathrm{d}^2\bar{C}}{\mathrm{d}Z^2} + \frac{V_{\text{eff}}}{D}\frac{\mathrm{d}\bar{C}}{\mathrm{d}Z} - \frac{S}{D}\bar{C} = -\frac{C_0}{D}.$$

Similarly, the interface (Eq. (4)) and far field (Eq. (5)) boundary conditions can be transformed as

$$\frac{\mathrm{d}\bar{C}}{\mathrm{d}Z} = -\frac{V_{\text{I}}}{D}(1-k)\bar{C} \quad \text{in } Z = 0,$$

$$\bar{C} = \frac{C_0}{S} \quad \text{in } Z = \infty.$$

The solution to this simple differential equation is of the form

$$\bar{C} = A\mathrm{e}^{-aZ} + \frac{C_0}{S},$$

where

$$a = \frac{1}{2}\frac{V_{\text{eff}}}{D} \pm \sqrt{1/D}\left(S + \frac{V_{\text{eff}}^2}{4D}\right)^{1/2}.$$

From the boundary conditions, we get

$$A = \frac{C_0}{S}\frac{q}{aD/V_{\text{I}} - q},$$

where $q = (1-k)$. Substituting the expression of a in A, we obtain

$$A = \frac{C_0}{S}\frac{qV_{\text{I}}\sqrt{1/D}}{\sqrt{1/D}[\frac{1}{2}V_{\text{eff}} - qV_{\text{I}}] + (S + V_{\text{eff}}^2/4D)^{1/2}}.$$

The Laplace transform of the composition thus becomes

$$\bar{C} = \frac{C_0}{S}\left\{1 + \frac{qV_{\text{I}}\sqrt{1/D}\mathrm{e}^{-1/2V_{\text{eff}}Z/D} \times \mathrm{e}^{-\sqrt{1/D}}(S + V_{\text{eff}}/4D)^{1/2}Z}{\sqrt{1/D}(\frac{1}{2}V_{\text{eff}} - qV_{\text{I}}) + (S + V_{\text{eff}}^2/4D)^{1/2}}\right\}.$$

We only kept the positive root of A in order to satisfy the far-field boundary condition. We are left with an expression exactly similar to that of Smith et al. (Eq. (25) in Ref. [6]) provided that q, k and R are, respectively, changed into

$$q' = q\Delta,$$

$$k' = 1 - q' = 1 - (1-k)\Delta,$$

$$R' = V_{\text{eff}}.$$

Using the inverse Laplace transform proposed by Smith et al., we get for the liquid-phase composition

$$C(Z,t) = C_0\left\{1 + \frac{q'}{2k'}\mathrm{e}^{-V_{\text{eff}}Z/D} \times \mathrm{erfc}[\tfrac{1}{2}\sqrt{1/Dt}(Z - V_{\text{eff}}t)] - \frac{1}{2}\,\mathrm{erfc}[\tfrac{1}{2}\sqrt{1/Dt}(Z + V_{\text{eff}}t)] + \frac{q'}{2}\left(\frac{1}{q'} - \frac{1}{k'}\right)\mathrm{e}^{(-q'V_{\text{eff}}/D)(Z + k'V_{\text{eff}}t)} \times \mathrm{erfc}[\tfrac{1}{2}\sqrt{1/Dt}(Z + \overline{2k'-1}V_{\text{eff}}t)]\right\}.$$

All that we now have to do to get the solid state segregation profile, given as Eq. (7) in the text, is to set $Z = 0$ in the above expression and multiply the result by the partition coefficient k. It should be noted that our expression for the liquid-phase composition has been checked to yield correct results in terms of interface and far-field boundary conditions, as well as steady-state value and initial conditions. It should also be noted that the Mathematica software on our PC has not been able to solve the starting differential equation.

References

[1] Q. Li, H. Nguyen Thi, H. Jamgotchian, B. Billia, Acta Metall. Mater. 43 (1995) 1271.
[2] R.J. Su, W.A. Jemian, R.A. Overfelt, J. Cryst. Growth 179 (1997) 625.
[3] S. Kuppurao, S. Brandon, J.J. Derby, J. Cryst. Growth 158 (1996) 459.
[4] W.A. Tiller, K.A. Jackson, J.W. Rutters, B. Chalmers, Acta Metall. 1 (1953) 428.
[5] R.G. Pohl, J. Appl. Phys. 25 (1954) 1170.
[6] V.G. Smith, W.A. Tiller, J.W. Rutter, Can. J. Phys. 33 (1955) 723.
[7] O.W. Memelink, Philips Res. Rep. 11 (1956) 183.
[8] D. Ma, W. Jie, S. Liu, W. Xu, J. Cryst. Growth 169 (1996) 170.
[9] S.H. Kim, S.A. Korpela, A. Chait, J. Cryst. Growth 183 (1998) 490.
[10] L. Nastac, J. Cryst. Growth 193 (1998) 271.
[11] J.A. Warren, J.S. Langer, Phys. Rev. E 47 (1993) 2702.
[12] B. Caroli, C. Caroli, L. Ramirez-Piscina, J. Cryst. Growth 132 (1993) 377.
[13] W. Huang, Y. Inatomi, K. Kuribayashi, J. Cryst. Growth 182 (1997) 212.
[14] J.A. Burton, R.C. Prim, W.P. Schlichter, J. Chem. Phys. 21 (1953) 1987.
[15] J.J. Favier, Acta Metall. 29 (1981) 197 and 205.
[16] F. Rosenberger, Fundamentals of Crystal Growth. I. Macroscopic Equilibrium and Transport Concepts, Springer, Berlin, 1979.
[17] D.T.J. Hurle, Crystal Pulling from the Melt, Springer, Berlin, 1993.
[18] J.P. Garandet, J.J. Favier, D. Camel, Segregation Phenomena in Crystal Growth from the Melt, Handbook of Crystal Growth, North-Holland, Amsterdam, 1994.
[19] C. Wagner, J. Metals 6 (1954) 154.
[20] L.O. Wilson, J. Cryst. Growth 44 (1978) 247 and 371.
[21] J.P. Garandet, J. Cryst. Growth 131 (1993) 431.
[22] F. Haddad, J.P. Garandet, D. Henry, H. Ben Hadid, J. Cryst. Growth 204 (1999) 213.

[23] J.J. Favier, L.O. Wilson, J. Cryst. Growth 58 (1982) 103.
[24] R. Hirsh, J. Comput. Phys. 19 (1975) 90.
[25] B. Roux, P. Bontoux, T.P. Loc, O. Daube, in: R. Rautmann (Ed.), Lecture Notes in Mathematics, Vol. 771, Springer, Berlin, 1980, p. 450.
[26] J.F. Thompson, Z. Vawarsi, C.W. Matsin, Numerical Grid Generation, Elsevier, Amsterdam, 1985.
[27] S. Kaddeche, H. Ben Hadid, D. Henry, J. Cryst. Growth 135 (1994) 341.
[28] S. Kaddeche, J.P. Garandet, C. Barat, H. Ben Hadid, D. Henry, J. Cryst. Growth 158 (1996) 144.
[29] Y. Inatomi, H. Miyashita, E. Sato, K. Kuribayashi, K. Itonaga, T. Motegi, J. Cryst. Growth 130 (1993) 85.
[30] A. Rouzaud, J. Comera, P. Contamin, B. Angelier, F. Herbillon, J.J. Favier, J. Cryst. Growth 129 (1993) 173.
[31] J.J. Favier, P. Lehmann, J.P. Garandet, B. Drevet, F. Herbillon, Acta Mater. 44 (1996) 4899.
[32] L. Helmers, J. Schilz, G. Bähr, W.A. Kaysser, J. Cryst. Growth 154 (1995) 60.
[33] L. Helmers, J. Schilz, G. Bähr, J. Cryst. Growth 165 (1996) 381.
[34] C.J. Chang, R.A. Brown, J. Cryst. Growth 63 (1983) 343.
[35] A. Rouzaud, D. Camel, J.J. Favier, J. Cryst. Growth 73 (1985) 149.
[36] Q. Xiao, S. Kuppurao, A. Yeckel, J.J. Derby, J. Cryst. Growth 167 (1996) 292.